Disclaimer

This note has not been internally reviewed by the DØ Collaboration. Results or plots contained in this note were only intended for internal documentation by the authors of the note and they are not approved as scientific results by either the authors or the DØ Collaboration. All approved scientific results of the DØ Collaboration have been published as internally reviewed Conference Notes or in peer reviewed journals.

The Performance and Physics Potential of the D-Zero Detector Operating at the SSC

D0 Note 1018
Oct. 10, 1990

W. Guryn, Brookhaven National Laboratory
N. Graf and T. Murphy, Fermilab
J. Womersley and J. Ohnemus, Florida State University
M. Fortner and D. Hedin, Northern Illinois University

This report considers the performance of the D-Zero detector operating at the SSC. It assumes that D-Zero has been upgraded to operate efficiently at $\sqrt{s}$ = 1.8 TeV and L = 10^{32}cm^{-2}sec^{-1} and that the detector is then moved essentially as is to the SSC. The physics capabilities of such a detector are outlined assuming an integrated luminosity of 1 fb^{-1}. Finally, an assembly scenario is discussed.

This report will not directly address the desirability of moving D-Zero to the SSC. It is clear that a detector with the parameters of D-Zero would be adequate for a good amount of physics at the SSC; nonetheless the new detectors now being proposed would have significantly greater capabilities. Thus a decision to move D-Zero to the SSC would need to be based on the Fermilab and SSC accelerator schedules, the construction schedules of the new SSC major detectors, the availability of an SSC interaction region for D-Zero, the cost of the move, whether adequate personnel resources exist, and other such factors which are presently beyond our ability to address.

1. D-Zero Detector Performance

The D-Zero detector[1] will take full advantage of the physics potential of the Fermilab proton-antiproton collider. Its design emphasises the measurement of electrons, muons, photons, jets, and neutrinos (through the missing energy). The detector (figure 1) has three major hardware systems: calorimetry, muon detection, and central tracking, which together allow complete characterization of most $p\bar{p}$ collision events. The tracking system consists of drift chambers to measure particle trajectories and transition radiation detectors to aid in electron identification. Surrounding this is an uranium-liquid argon calorimeter which provides superior energy resolution, particle identification, hermeticity, and is exceptionally stable and radiation resistant. The muon system consists of five magnetized iron toroids and associated drift chambers and covers 98% of the full solid angle.

The D-Zero detector, as initially designed, will be able to operate at luminosities up to about 10^{31}cm^{-2}sec^{-1}. Increasing the luminosity to 10^{32} will require upgrading some of the components. Possible scenarios have been discussed[2] and a specific upgrade proposal will be developed during the next year. The calorimeter and muon systems were designed with the intensity upgrade in mind

and so will only require changes to the front end and trigger electronics. Major changes, however, will have to be made to the central tracking systems.

This report will discuss the performance of the upgraded calorimeter and muon systems operating at $\sqrt{s} = 40$ TeV. We will also discuss the trigger and data acquisition systems. The D-Zero collaboration has not finalized the central tracking upgrade design for operating at higher luminosities and we will not discuss any possible SSC scenario. We do note that the duty cycle of the SSC is preferable to that of the Fermilab collider and so tracking, for the same luminosity, should be somewhat better at the SSC. We do not feel that the conclusions we present in this report depend on the details of the tracking system which is eventually proposed and constructed for the D-Zero upgrade.

1.1 The D-Zero Calorimeter at $\sqrt{s} = 40$ TeV

The D-Zero calorimeter provides uniform, full depth coverage for electron and hadron energy and position measurements using liquid argon as an ionization detection medium and uranium plates (copper or stainless steel in the leakage section) for the absorber. Three separate calorimeter vessels cover the region down to 1 degree with respect to the beam, as shown in cross section in figure 1.2. The calorimeter is compact, linear, has good energy resolution, and represents in our judgment the best calorimeter system at any presently operating collider in terms of hermeticity and thickness. The readout towers are finely segmented to give a detailed measure of energy deposition pattern: the readout pads cover $\Delta\eta \times \Delta\phi = 0.1 \times 0.1$ (0.05×0.05 near the EM shower maximum) and are in 7 or 8 longitudinal segments (4 EM, of 2,2,7 and 10 X_0 followed by 3 or 4 hadronic each $\geq 1\lambda$). The argon gap width is 2.3 mm, yielding a time for full charge collection of about 400 nsec. Liquid argon calorimetry has the advantage for the high luminosity upgrade that it is radiation hard, and that the calibration for the system is simply achieved. The calorimeters have been built with the upgrade in mind, in that the cell capacitances and readout cable impedences are constrained so as to make fast readout possible. Preamplifiers are mounted outside the cryostats, but as close as possible to the modules. Modifications to the calorimeter electronics for very high luminosities are being considered since the mix of contributions from electronics noise, uranium noise and the effect from deposits due to overlapped events will change.

1.1.1 Electrons

We imagine that the primary use for the D-Zero calorimeter at the SSC would be for electron energy measurement and identification. We have already demonstrated the performance of the EM calorimeter for single high energy electrons (150 GeV) in the Fermilab test beam[3], and obtain an energy resolution for normal incidence of

$$\frac{\sigma}{E} = \left(\frac{0.16^2}{E} + 0.003^2\right)^{\frac{1}{2}} \text{E in GeV.}$$

Electrons will therefore be well-measured at high energies. Using the D0GEANT Monte Carlo, we predict that for real electrons with non-normal incidence, smeared vertex position and central detector material present, the energy resolution is roughly constant at 4% over the range $0 < |\eta| < 3$ for 100 GeV E_T electrons and 12% for 15 GeV E_T electrons, as shown in figure 1.3. The poorer resolution seen in this figure hear $\eta = 0.8$ is due to the transition between the central and end cryostats.

Electron identification in D-Zero is done starting with isolated EM clusters in the calorimeter. A covariance matrix is used to derive a chi-squared for the clusters to be due to electrons, and to predict the energy lost because of cracks and/or uninstrumented material and the impact position. This technique has been demonstrated to achieve a pion rejection factor of 500 (with an electron efficiency between 85 and 90%) from 10 to 150 GeV. We see no reason why this philosophy will not continue to work for higher energy electrons, especially as the finely segmented longitudinal layer structure of the D-Zero calorimeter means we will not suffer when TeV-energy electron showers begin leaking into the hadronic section. Also, D-Zero currently uses a TRD for additional e/π separation. All upgrade scenarios also include either a new TRD or a pre-shower device, with typical pion rejection factors of 10-100.

Electron acceptance for D-Zero is influenced by three effects:

- In the central calorimeter, there are azimuthal cracks between adjacent electromagnetic modules;
- Between the central and end calorimeters there is a region with no EM coverage.
- Above $\eta = 3$ the drift chamber system fails to give good tracks so electron discrimination from pi-zeros is not possible.

Using the D0GEANT Monte Carlo we estimate a geometrical electron acceptance of 80% for 15 GeV E_T to 100 GeV E_T electrons generated uniformly in $-3 < \eta < 3$ and $0 < \phi < 2\pi$. The acceptance as a function of pseudorapidity is shown in figure 1.4. This geometrical acceptance must be multiplied by an estimated 85% efficiency factor for the electron finding algorithm.

1.1.2 Jets and Missing E_T

The calorimeter thickness ("live" and total) is shown in figure 1.5 as a function of pseudorapidity and ranges from about 6.5 interaction lengths at $\eta = 0$ to 8.5 at $\eta = 4.0$. The calorimeter energy resolution for jets is typically 10% for 100 GeV E_T jets over the central, $|\eta| < 1$, region, rising to 15% in the forward region. To determine whether there is any need to add backing calorimetry outside the present D-Zero detector, we have compared the performance of the present arrangement for jets of fixed $E_T = 100$ GeV and 2 TeV. As shown in

figure 1.6, the 2 TeV E_T jets are actually better measured: the fractional energy resolution is about 4% for $|\eta| < 1$ and 5% forward. The improved resolution results from higher average particle energy. At the higher energy, greater fluctuations in leakage energy from the calorimeter might be expected. Figure 1.7 shows that this is not significantly so: the energy lost to leakage, and nuclear processes (from D0GEANT simulation) is very similar at $E_T = 2$ TeV to that at 100 GeV. It does not therefore seem worthwhile to invest in additional calorimetry (backing calorimeters have been suggested), though the further study of jet and missing E_T resolution requirements is certainly needed.

1.1.3 Noise and Pileup

New calorimeter electronics will need to be procured to operate at the Tevatron with luminosities of 10^{32}. A working group within the D-Zero collaboration is currently attempting to define our preferred solution. It is likely that such a system would involve

- New preamplifiers with two FET's in parallel and differential cable drivers;
- New shaping hybrids (BLS's) with symmetric shaping and a 500 ns base-to peak time (the current system is unipolar with 2.3 μs shaping time).
- An analog delay to allow the trigger to be preformed.

The noise in this system, per channel, is estimated to be about 50 MeV from uranium decays (compared with 100 MeV in the current D-Zero) and 71 MeV electronic noise (compared to 50 MeV now).

Additional noise will result from pileup of minimum bias events (and occasional QCD jet events) occuring before or after the triggered event of interest. This is unavoidable because of the relatively slow drift time of liquid argon compared with the 16 ns bunch crossing time. As an estimate, we may scale from the values for $\sqrt{s} = 1.8$ TeV given in reference 2 and obtain pileup noise per 0.1×0.1 tower at the SSC of 375 MeV ($L = 10^{32}$) and 1.2 GeV ($L = 10^{33}$). Similar results are obtained by scaling the calculations of Cleland[4] for the EMPACT liquid argon calorimeter with 400 ns drift time and 0.32×0.32 towers. This magnitude of pileup noise seems manageable, though it is potentially the largest source of noise in the system.

1.1.4 Radiation Hardness

The environment at the SSC will give high radiation doses to the D-Zero calorimeter because of its small radius and its high rapidity coverage. For luminosities of 10^{32} and 10^{33} respectively, we expect maximum ionizing dose rates on the order of 10 Mrad and 100 Mrad per year.[5] This maximum dose occurs in the end EM calorimeters at $\eta = 4.0$, and the dose is much less at smaller rapidities. Despite the high dosage, we expect no problems because the entire device is intrinsically very radiation hard. It is built only of metal, argon and

G-10, and contains no active plastic or silicon structures. There may be some legitimate concern about the epoxy glues used in some parts, but we trust that several years of operation of this calorimeter at high rates at the Tevatron, and additional tests to be carried out for the liquid argon subsystem for the SSC, will have demonstrated this required level of radiation hardness for the complete system.

1.1.7 Calorimetry conclusions

The D-Zero calorimeter would be an adequate SSC calorimeter for a variety of physics processes. This preliminary study has indicated that it would perform well at the higher energy, and no insuperable objections exist to its operation at the SSC.

1.2 The D-Zero Muon System at $\sqrt{s} = 40$ TeV

The D-Zero muon system consists of magnetized iron toroids (1 to 1.5 m thick) surrounding the calorimeter and 170 proportional drift tube chambers covering the region above about 5 degrees. The chambers are arranged in three layers with one between the calorimeter and the toroids and two outside the toroids. Most chambers have 10 cm drift cells and either three (for the outside chambers) or four measurement planes. At small angles, the chambers have 2.5 cm cells and six planes per layer. Finally, a plane of scintillation counters covers the ceiling to aid in rejecting cosmic ray muons. Extending this coverage to all sides is currently under consideration as part of the Tevatron upgrade.

As seen in figure 1.8, the total thickness of absorber in the calorimeter and muon toroids is about 14 λ in the central region and 18 λ in the forward. This is more than enough for rejecting punchthroughs at SSC energies.[6] The muon momentum resolution is limited by multiple scattering to be greater than 18%. Figure 1.9 gives the momentum resolution as a function of p_T for various angles. Muon rates at the SSC have been estimated elsewhere.[6] Raw muon rates will vary from 5 kHz ($|\eta| < 1$) to about 200 kHz ($2 < |\eta| < 3$). In addition, there will be a large rate at smaller angles due to hadronic interactions in material such as the beam pipe and low-β quadrupoles. Calculations performed for the D-Zero geometry at Fermilab indicate that the low-β quads are the largest source, producing about 5 particles per $p\bar{p}$ interaction in the measuring station furthest from the interaction point. The SSC quadrupoles are at least 20 m (further for the low-luminosity halls) from the interaction point compared to 8 m at Fermilab. As such, we anticipate that the rate from this source is no worse at the SSC than at Fermilab and that the occupancy level is acceptable.

As discussed in Section 3 below, a possible SSC construction scenario would have the muon toroids assembled out of new material while D-Zero continues to operate at Fermilab. With this flexibility, we would consider making limited changes to the layout of the muon system. First, we would extend the coverage of the end toroids by about 1 m in order to eliminate the central-end gap seen

at 40 degrees in figure 1.8. This would increase the iron from about 5000 tons to 5900 tons. Also, as seen in figure 1.9, the contribution to the resolution from measurement errors becomes equal to that from multiple scattering at around p_T of 300 GeV. Doubling the outside lever arm increases this by two. This extended lever arm also raises the muon trigger p_T threshold to about 10 GeV/c. Implementing such an increase in lever arm would require about 40 additional 15 m^2 drift chambers (30% of the current area). We will assume in this report that both the increase in iron and lever arm would be implemented.

1.3 The D-Zero Trigger and Data Acquisition System at $\sqrt{s} = 40$ TeV

The D-Zero trigger consists of two stages. The first stage (level 1) uses dedicated hardware to produce a trigger. The level 1 trigger directs the VME-based data acquisition system to build the event, including digitization of calorimeter and muon signals, and formatting data from the central tracker and trigger framework. The digitized data is transferred to a MicroVAX farm where a level 2 trigger makes further cuts before writing the event to tape. Both the level 1 and 2 have a single stage of buffering to reduce deadtime.

The current level 1 trigger takes information from coarse-grained electromagnetic and hadronic calorimetry and hits in the muon system to form a trigger within 2.6 μsec after beam crossing. Proposed upgrades to D-Zero would add analog delay lines and faster trigger elements to reduce the time to form a trigger to 1.6 μsec. The level 1 trigger also supports a level 1.5 refinement of the trigger that can abort the event digitization after about 10 μsec using improved detector information and the global event topology.

The bandwidth of the current data aquisition system can support an average event rate of 200 Hz into the Microvax farm, with a peak event rate of 400 Hz. Upgrades to D0 will improve this to an average event rate of 500 Hz with a peak event rate of 1000 Hz. With this limitation, the level 1 trigger needs to reduce the event rate to 500 Hz. The output of level 2 is restricted to the speed events can be written to tape. It is planned for the level 2 trigger to reduce the event rate to 1-10 Hz.

Calorimeter-based triggers all have adjustable thresholds which can be raised so that the event rate is below the data taking limits. For example, requiring an electromagnetic tower with E_T greater than 35 GeV gives a 100 Hz rate. Furthermore, the calorimeter trigger is flexible enough to assign different threshold to different trigger towers, so that only those regions of the detector need to have the threshold increased. The calorimeter trigger also features multiple thresholds for each tower, permitting lower threshold energies for triggers involving multiple trigger elements such as e-μ.

However, the first level muon trigger, even with increased lever arms, has a p_T threshold of 10 GeV/c. The single muon muon rate will be 1000 Hz for $|\eta| < 2$ (100 Hz for $|\eta| < 1$). The single muon trigger rate exceeds the 500 Hz

bandwidth, but most interesting physics channels can be triggered using combinations of hardware triggers (such as di-muon, e-μ, or μ-missing energy). Studies involving triggering on top decays at Fermilab energies indicate that the current triggering options are acceptable for higher mass channels.

2. Survey of Physics Topics

This section surveys some of the physics capabilities of the D-Zero detector operating at the SSC. We will assume $\sqrt{s} = 40$ TeV and an integrated luminosity of 1 fb^{-1}. There a variety of references for these topics. We have used EHLQ,[7] the 1987 Berkeley workshop, and the expressions of interest of SDC as our primary sources.

We have only done a limited amount of simulation of the physics channels described. The reactions $Z' \rightarrow ee$ and $H \rightarrow ZZ \rightarrow 4e$ have been simulated using the complete D-Zero GEANT Monte Carlo and serve as examples of the estimated reconstruction efficiency. The SDC in their EOI have tried to include detector and analysis efficiencies in their rate calculations. If we compare D-Zero to their proposed design, the electrons will have similar resolution and geometric coverage but D-Zero will have a 70% efficiency compared to SDC's estimated 90%. Muons will have similar backgrounds and efficiency (both about 90%) with D-Zero having slightly better coverage and SDC much better resolution.

2.1 Top quark studies

The detection and reconstruction of $t\bar{t}$ events using the D-Zero detector has been discussed elsewhere.[8] At the SSC, the production cross section is large enough to allow both discovery for masses above 250 GeV and systematic studies once discovered. For a top mass of 250 GeV, the production cross section is 1.5 nb. An integrated luminosity of only 10 pb^{-1} is needed for top discovery via the $t\bar{t} \rightarrow (e\nu b)(\mu\nu b)$ channel. For 1 fb^{-1}, there will be about 30,000 eμ events and about 400,000 lepton plus multi-jets events. The eμ channel is expected to have small background but the two neutrinos limit how well the event can be reconstructed. Thus the mass can only be inferred from the production cross section.

Studies have shown that the $t\bar{t} \rightarrow (l\nu b)(q\bar{q}b)$ channel is reconstructible with the D-Zero detector thereby allowing a direct determination of the mass. For higher top masses, difficulties will arise in assigning the correct jets when forming invariant mass plots. Tagging the b-jets would improve the cleanliness of the signal and the determination of the top mass. Low p_T muons will tag about 30% of the b-jets. The addition of a silicon vertex detector as part of the inner tracking upgrade would also aid in this tagging and is currently under consideration. One can also use topological selections to reduce the jet assigning combinatorics. This gives a more precise mass measurement but with lowered efficiency, which, given the large cross section, is acceptable at the SSC.

Top decays can also be used to search for charged Higgs through the decay $t \rightarrow H^{\pm}b$ and subsequent decay of the Higgs to $\tau^{\pm}$. Direct observation of this decay would be better with a central magnetic field. However, D-Zero, by measuring the top semi-leptonic branching ratio would infer the existence of non-standard decay channels.

2.2 New W's and Z's

The existence of new gauge bosons is predicted by many models. However, the couplings depend on the model and there are no predictions for the masses. Eichten[9] estimates that, for an integrated luminosity of 1 fb^{-1}, the discovery limits will be 4.2 TeV for a new Z and 4.6 TeV for a new W. This is based on producing about 15 $Z' \rightarrow ee$ events and 50 $W' \rightarrow e\nu$ events with $|y_{Z,W}| < 1.5$. The background from Drell-Yan is estimated to be about 10^{-4} and should not pose a problem. The electron and missing energy resolution and the electron identification of D-Zero are more than adequate for discovery[10] and would also give a very good measurement of the Z' width. The muon channels would serve to confirm any electron signals. Studies[11] indicate that by using the missing energy in combination with the muon momentum measurement, the $\mu - \mu$ mass resolution will be less than 30% even at the higher Z' masses. However, the muon momentum resolution will probably limit the ability to measure charge asymmetries should a Z' be discovered.

We have performed a reasonably detailed study of the $Z' \rightarrow ee$ channel. The GEANT-based full detector Monte Carlo was used. Two hundred events were generated using ISAJET, and the electrons run through the detector simulation and a preliminary version of the D-Zero electron-finding algorithm. As shown in figure 2.1, the resulting ee mass peak is easily reconstructed with a resolution of 3.6% and 73% acceptance. This acceptance may be somewhat over-estimated as there were no underlying events included in the simulation.

2.3 Production of Higgs bosons

One of the primary goals of the SSC is to explore the mechanism which produces symmetry breaking in the gauge sector. The Higgs mechanism is one possible scenario though details such as the number and masses of the physical Higgs bosons cannot be predicted. We will assume the simplest scenario with a single Higgs coupling primarily to W- and Z-pairs for the mass region of interest.

For $M_H < 2M_Z$, the reaction $H \rightarrow ZZ^*$ with one Z off the mass shell appears to be reconstructible with adequate background rejection. This reaction is suppressed for lower Higgs masses. SDC estimate that, for 10 fb^{-1}, a lower limit of 120 GeV can be reached. We have not done a detailed estimate for D-Zero at lower luminosity but it appears that the mass range above 160 GeV would be detectable.

For $M_H > 2M_Z$, the Higgs will decay primarily into W- and Z-pairs. Table 2.1 gives the expected number of events for top masses of 100 and 200 GeV.

The $ZZ \rightarrow 4l$ with $l = e, \mu$ will give the cleanest signal. Studies[12] indicate that, using the dilepton mass, isolation, and p_T balance, the Z + jet background can be eliminated even for lepton momentum resolutions of 20%. For example, figure 2.2 compares the ratio of p_{TZ1}/p_{TZ2} with $p_{TZ1} < p_{TZ2}$ before and after isolation cuts. A cut on this ratio at 0.5 reduces backgrounds from both $b\bar{b}$ and $t\bar{t}$ events with a minimal loss in signal. The remaining background is entirely due to Z-pair continuum and is estimated to be about 20% of the Higgs signal for $m_H = 400$ GeV.

The significance of the Higgs signal to the continuum Z-pair background then depends on the number of events and the 4-lepton mass resolution. Table 2.2 gives the mass resolution assuming a perfect detector and also assuming the electron and muon energy resolutions expected in D-Zero. These values used the Z mass as a constraint on lepton pairs. This estimate for the 4 electron channel gives a measured width within 10% of the natural width; a more detailed detector simulation carried out for $m_H = 400$ GeV suggests that the actual obtainable width with a real calorimeter may be 50% greater than the natural width. The muon channels will have wider signals with the $ee\mu\mu$ channel having a width from (25-50)% wider and the 4 muon channel being (35-90)% wider than the natural width for Higgs masses from 300 to 600 GeV. For a Higgs mass of 400 GeV and a 1 fb^{-1}, about 30 4-lepton events (5-7 4e, 10 4μ and 15 2e2μ) would remain after all acceptance and efficiency losses. The mass resolutions shown in Table 2.2 will degrade the S/N from 5 to 3.1 (or 4.1 if the 4μ channels is ignored). The 30 Higgs events would then give a 4.8 σ enhancement over the continuum.

The electron efficiency was calculated using the full GEANT-based calorimeter simulation. $H \rightarrow ZZ \rightarrow 4e$ events ($m_H = 400$ GeV). were generated with ISAJET and the electrons showered in the calorimeter; electrons were then found with a preliminary version of the electron-finder code and electron pair masses reconstructed (an electron p_T cut of 10 GeV was used). As shown in Figure 2.3(a), the Z mass could be reconstructed with a resolution of 7.5 GeV. Figure 2.3(b) shows the p_T spectrum of the Z. Electron pairs with masses within 3 standard deviations of m_Z were then constrained to m_Z and the ZZ mass was reconstucted. The ZZ mass spectrum is shown in figure 2.3(c). The resolution on the Higgs mass is 30 GeV and the acceptance after all effects is about 30%. If a harder electron p_T cut (20 GeV) is used, this acceptance drops to about 25%. These events had no underlying event included. To investigate the possible reduction in electron efficiency from lack of isolation that might result, complete events (Higgs plus underlying event) were generated using HERWIG and simulated using a "toy" calorimeter. Figure 2.4 shows the ZZ mass spectra for 200 and 400 GeV Higgs using this simulation. The efficiencies are very similar to the more detailed calorimeter simulation without the underlying event, indicating no significant loss of signal from lack of isolation. Figure 2.5 gives an estimate of the ZZ continuum background to the 4e signal.

We have also studied the $H \rightarrow ZZ \rightarrow l^+l^-\nu\nu$ channel. This decay mode is of interest because it offers potentially higher rates than corresponding all-charged-lepton modes (due to the larger branching ratio for $Z \rightarrow \nu\nu$). This must be placed against the potential problems of large backgrounds from physics processes such as Z+jets and continuum ZZ production. Initial studies have been performed by Forden[13] for EMPACT and by Barnett and Hinchliffe[14] for SDC.

The signal for this process is two charged leptons (electrons or muons) reconstructed to the Z mass, back-to-back with missing p_T. The invariant mass of the Higgs boson cannot of course be reconstructed from these events. Instead one may use the observed unbalanced p_T of the Z boson which forms a Jacobian peak at about half the Higgs mass. The background to this peak comes mainly from Z+jets events where one or more jet was mismeasured leading to unbalanced p_T. The ability to see signal above background events is therefore quite a stringent test of the missing p_T resolution of the detector. Forden's study indicates that for the case of D-Zero, where jet measurement is only fully hermetic up to $\eta \sim 3$ (because beyond that shower energy leaks into the beampipe), the signal may be very hard to see in missing p_T alone (see figure 2.6). It is possible to construct a transverse mass m_T from the ee pair and the missing p_T vector. Using hard cuts to reject the background from Z + jets ($|\eta_Z| < 2$, $p_T(ee) > 150$ GeV, $p_T(miss) > 150$ GeV) and realistic D-Zero electron and hadron calorimeter resolutions, one can obtain a good signal to background ratio for a 400 GeV Higgs (see figure 2.7). It may be possible to use additional cuts and selections to aid in extracting a signal. For example, Barnett and Hinchliffe suggest cutting events with a large azimuthal angle between the Z and the highest transverse-momentum jet, and events without forward high-P_T jets. Further study of this process is therefore needed before we can state definitely whether it is within the capability of D-Zero.

2.4 Pair production of gauge bosons

Table 2.3 gives the number of events predicted in a variety of continuum ZZ, WZ, Wγ, and $Z\gamma$ channels. $W\gamma$ and $Z\gamma$ channels should be readily identified.[1] The reconstruction of WZ and ZZ events with both gauge bosons decaying leptonically will give clean signals. As with Higgs events, QCD background events can be rejected by using lepton isolation, dilepton mass and p_T, and p_T balance. Including a 50% efficiency, the roughly 500 $WZ \rightarrow (l\nu) + (ll)$ can be used to measure the production cross section versus M_{WZ} with about 1% of the events having M_{WZ} greater than 1 TeV. Studies of W^+/W^- differences and polarizations will be limited by statistics. The 50-100 reconstructed $ZZ \rightarrow 4l$ events can also be used to measure the production cross section. In addition, there will be six times more $ZZ \rightarrow ll\nu\nu$ events. Separating these events from the Z + jet background is difficult but would certainly be attempted.

3. Installation of the D-Zero Detector at the SSC

This section discusses a scenario and its associated costs for installing the

D-Zero detector at the SSC. We assume that the platform and the muon iron will be constructed from scratch with new material. This can be done while D-Zero is operating at Fermilab. The muon chambers and the new central tracking would be shipped as is. With the proposed SSC muon system, about 40 new PDTs will need to be built. They could be of a new design and could, for example, be the initial chambers from the production line of one of the new SSC detectors. The most important question is how to move the calorimeter and, in particular, do they have to be disassembled. There are two open questions related to this. The first is can items of the size and tonnage (about 300 mt) of the three assembled calorimeter units be shipped from Batavia to Waxahachie. If they can, then will this cause greater damage to them then if they were disassembled, shipped, and then reassembled.

We have investigated the possibility of moving assembled cryostats from the D-Zero to the SSC. There is a clear advantage in doing so since one can avoid a very time and manpower consuming series of tasks: opening of the cryostats, removal of the modules, testing, assembly and closure of the cryostats. From what we have learned it is feasible to move all three D-Zero cryostats with modules in them.

Loads of the weight and sizes comparable to our calorimeters have been moved successfully already. The transport is a combination of road using a specially designed truck, and on water via barge.[15] Transport from Fermilab to the SSCL may have the advantage of only having to utilize truck transport within two states (Illinois and Texas) while using barge transport for the remainder. Details of the transport in terms of cost and routing are shown in Table 3.1. The cost estimate is very reasonable, $500,000, which covers the transportation from the D-Zero parking lot to the SSC site. Additional equipment to remove the fully loaded cryostats has not been included in the above price but it is not expected to be difficult and will require equipment whose cost is comparable to the $500,000 required for the move. In summarry, we conclude that moving the fully assembled calorimeters of the D0 experiment can be done and it will cost no more than $1,000,000.

Table 3.2 gives an estimate for the construction schedule of the detector presented in this report.[16] This table assigns the time $T0$ to be the last day of data taking of D-Zero at Fermilab. We assume eighteen months from the beginning of the hall construction to beneficial occupancy, thirty-six months for the heavy iron work of the platform and toroids, and twelve months to install the muon and central tracking chambers. We estimate beginning the iron work twenty-four months before the ending of D-Zero's Fermilab operations. The critical path is the calorimeter with the length of time dependent on the transport scheme. Here we assume completely disassembling, shipping, and then reassembling and testing the modules. This gives a total of thirty-six months. This assumes that much of the work proceeds in parallel which will require sufficient clean room assembly space

at the SSCL.

A preliminary cost estimate for installing D-Zero at the SSC is given in Table 3.3. It uses the October, 1989 D-Zero cost estimate as a starting point. The figures include EDIA but do not include contingency. They also do not include the cost of the collision hall and its supporting structures. As stated above, it is assumed that the platform, its associated supporting equipment (like cryogenics), and the muon toroids would be duplicated at the SSC. Other supporting equipment, such as high and low voltage power supplies, would continue in use. The cost of additional muon chambers simply scales from the current chambers with these chambers possibly being produced in conjuction with another SSC muon detector.

We have estimated the cost of disassembling, transporting, and then reinstalling the D-Zero detector by starting from the $4.1M cost of its initial installation at Fermilab. We have simply assigned the same figure for installation at the SSC, and then somewhat arbitrarily assigned half that value to disassemble the detector. As discussed above, a very preliminary estimate of moving the calorimeter gave a cost of less than $1,000,000. Our guess is that this will increase as more thought is put into it and so we have used $2,000,000 for the cost of moving the entire detector (excepting the support platform and iron toroids). Our current estimate then gives $11.9M for new equipment, $8.1M for installation, and $1M for administration, or a total of $21M (in FY90 dollars) to install D-Zero at the SSC.

References

1. D-Zero Design Report, Fermilab (1984). Muon system: C. Brown, et al., NIM, **A279**, 331 (1989); J.M. Butler, et al., NIM, **A296**, 122 (1990).

2. D. Buchholz, et al., Breckenridge upgrade report, also M. Tuts, report on Calorimeter electronics upgrade meeting, Fermilab, 12-13 June 1990.

3. M. Abolins et al., NIM, **A290**, 36 (1989).

4. W. Cleland, EMPACT Technical note.

5. D. Groom, in Proceedings of the Snowmass Summer Study, 1988.

6. D. Green and D. Hedin, FERMILAB-Pub-90/18, accepted by NIM.

7. E. Eichten, I. Hinchliffe, K. Lane, C. Quigg, Rev. Mod. Phys. **56**, 579 , 1984.

8. S. Abachi, et al., Top Group, Breckenridge 1989; P. Grannis, D-Zero Note 928, 1990.

9. E. Eichten, FERMILAB-PUB-85/178T.

10. J.S. Whitaker and N. Deshpande, Berkeley 1987.

11. Electroweak group, Breckenridge 1989.

12. I. Hinchliffe and E. M. Wang, Snowmass 1988; F. Paige, Tucson 1990; SDC EOI, May 1990.

13. G. Forden, in EMPACT EOI, May 1990, and private communication.

14. R.M. Barnett and I. Hinchliffe, LBL-28773, March 1990. see also reference 12.

15. It may also be possible to transport the calorimeter by rail. Movement of such a heavy load presents problems of weight, since most US railways are limited to a loading of approximately 30 tons per axle. Specialized vehicles meeting our requirements do exist: for example, General Electric's transformer division uses 12-axle rail cars capable of carrying 375-ton loads, measuring about 17 feet high, 10 feet wide and 20 feet long. The transformers are designed to mate to the framework of the car rather than simply being loaded on to a flat surface; nonetheless, it would probably be possible to design a simple girder structure that could carry a filled D0 cryostat on such a mounting. These cars travel as special movements rather than in regular trains and their speed is limited to 15 mph.

16. Site-specific Study of SSC Support Facilities for Four Generic Detector Designs, SSCL, July 1989. This report studied the construction of a greatly upgraded D-Zero detector.

17. The cost estimate for transporting the calorimeter was obtained by contacting Belding Engineering for rigging expenses, Press Express for motor transport expenses, and Midwest Marine Management for barge transport expenses. The costs do not include removal of the calorimeter from the D-Zero building.

Table 2.1 Estimated Higgs Decay Rates for 1 fb^{-1}

Higgs Mass	300	400	600
$H \to ZZ \to 4l$	250(108)	90(108)	25(54)
$H \to ZZ \to ll + \nu\nu$	1500	540	150
$H \to ZZ \to q\bar{q} + ll$	6000	2100	750
$H \to WW \to q\bar{q} + l\nu$	33000	11000	4000
$l = e, \mu$			
m_{top} = 100 (200) GeV			

Table 2.2 $H \to ZZ \to 4l$ Mass Resolution (sigma GeV)

Higgs Mass (GeV)	300	400	600
perfect dp/p	9.4	18.3	57
4 e	9.8	18.9	57
ee$\mu\mu$	14.1	28	69
4 μ	15.8	35	80

Table 2.3 Pair Production of Continuum Gauge Bosons

Channel	Events for 1 fb^{-1}
$WZ \to l\nu + ll$	1000
$ZZ \to ll + \nu\nu$	600
$ZZ \to 4l$	100
$Z\gamma \to ll + \gamma$	1000
$W\gamma \to l\nu + \gamma$	1000
$M_{W\gamma, Z\gamma} > 200$ GeV	
$l = e, \mu$	

Table 3.1 Calorimeter Transportation Cost Estimate (FY90K$)[17]

Work Performed	Cost
Load caloriemter onto truck in D0 parking lot	27
Transport from Fermilab to Lemont, Illinois barge terminal and from Houston barge terminal to SSCL	300
Unload truck and transfer to barge	27
Barge from Lemont, Illinois to Houston, Texas ($14.50/ton)	22
Unload barge and transfer to truck	27
Miscellaneous: truck, crane, barge demurrage/detention	100
total	503

Table 3.2 Assembly Schedule Estimate

Item	begin	end (months)
Collison hall	$T0$ - 42	$T0$ - 24
Platform and toroids	$T0$ - 24	$T0$ + 12
Disassemble and move	$T0$	$T0$ + 12
Install muon and inner tracking	$T0$ + 12	$T0$ + 24
Assemble/test calorimeter	$T0$ + 8	$T0$ + 24
Install calorimeter	$T0$ + 24	$T0$ + 36

Table 3.3 Cost Estimate (FY90K$)

Muon toroids	5,100
New muon chambers	1,500
Associated equipment	5,300
Disassembly	2,000
Transportation	2,000
Installation	4,100
Administration	1,000
Total	21,000

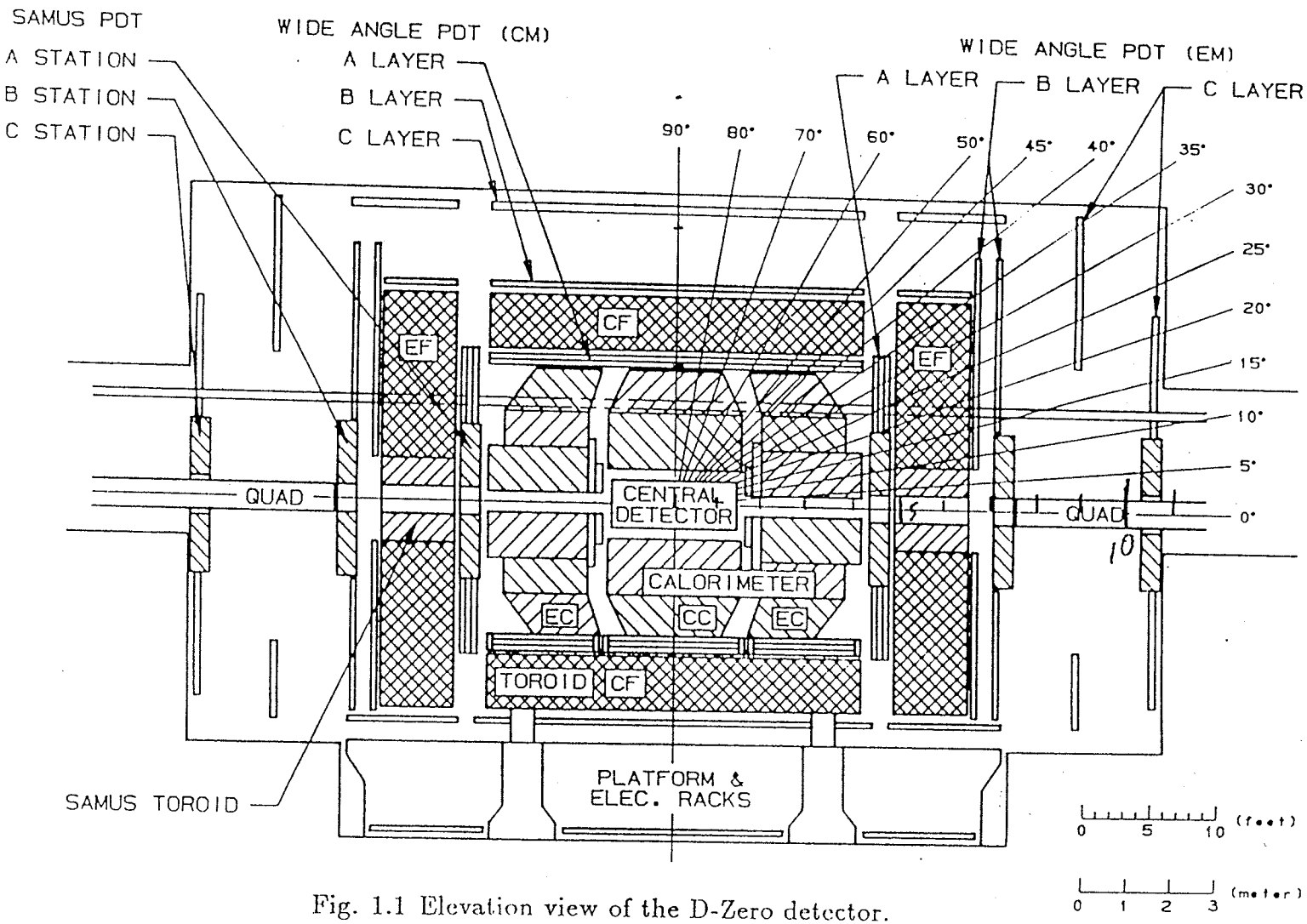

Fig. 1.1 Elevation view of the D-Zero detector.

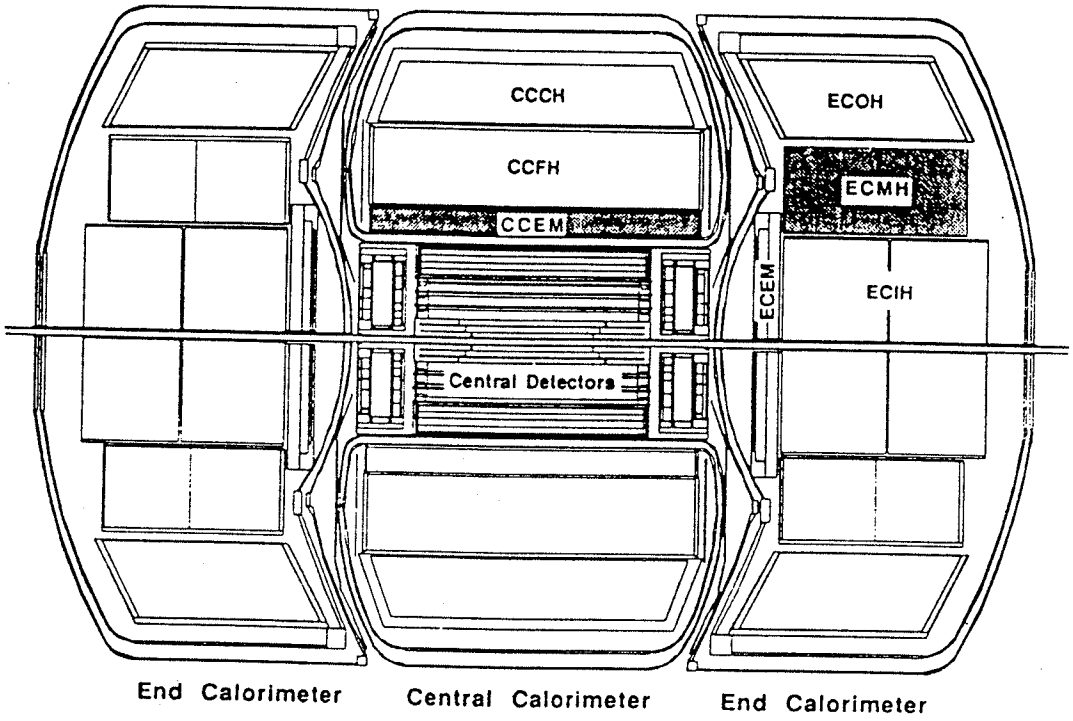

Fig. 1.2 Cross sectional view of the D-Zero calorimeter.

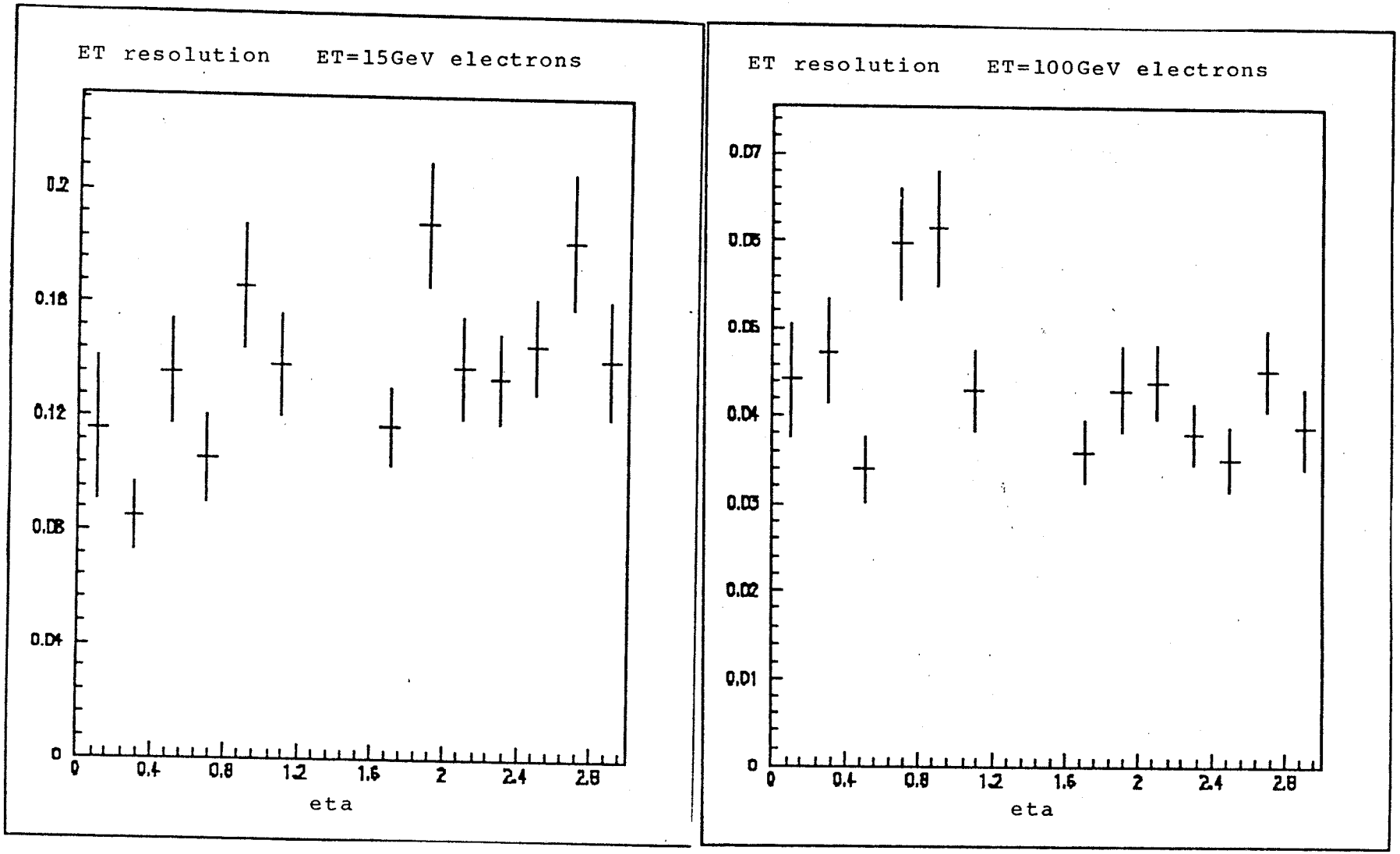

Fig. 1.3 Electron energy resolution as a function of pseudorapidity.

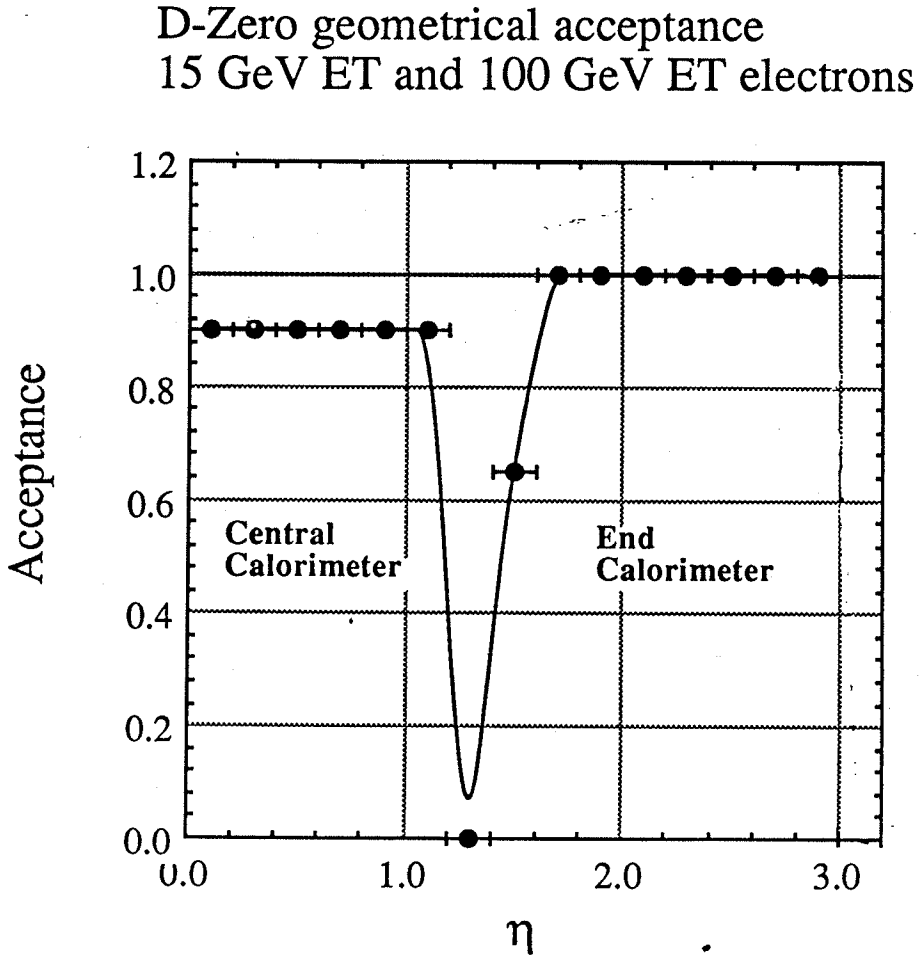

Fig. 1.4 Electron acceptance as a function of pseudorapidity (the starting vertex was smeared with a width in z of 7 cm).

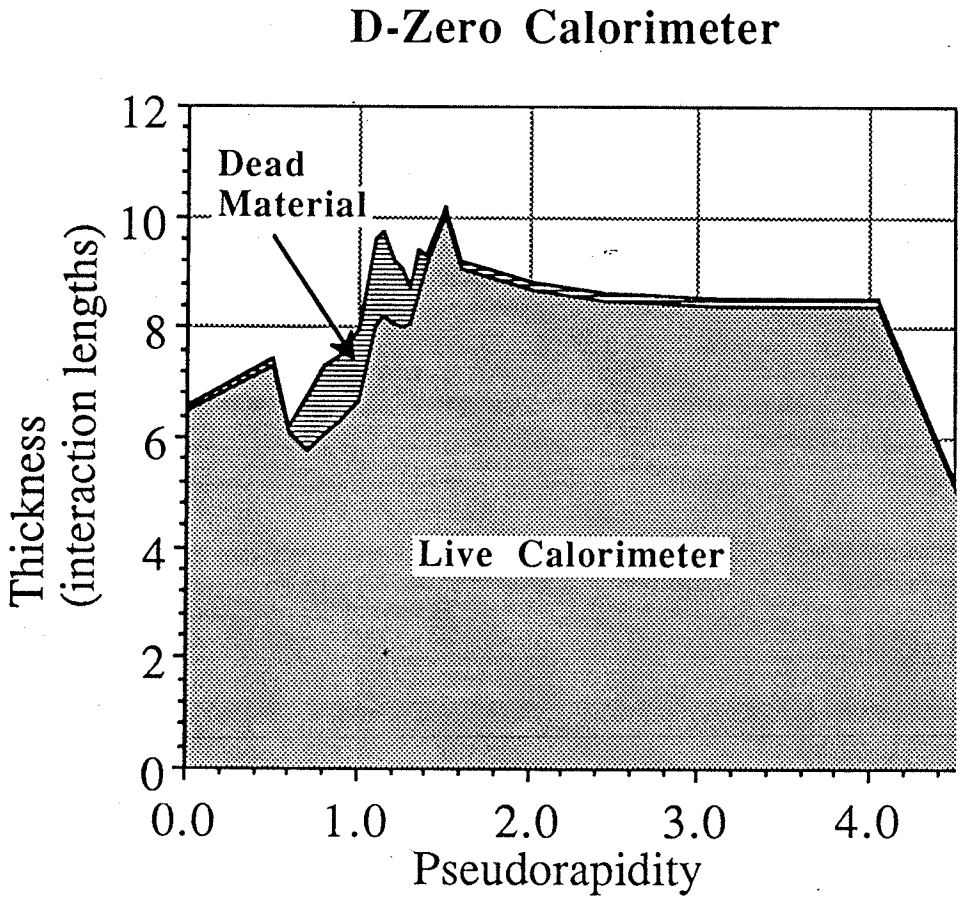

Fig. 1.5 Thickness of the D-Zero calorimeter in interaction lengths.

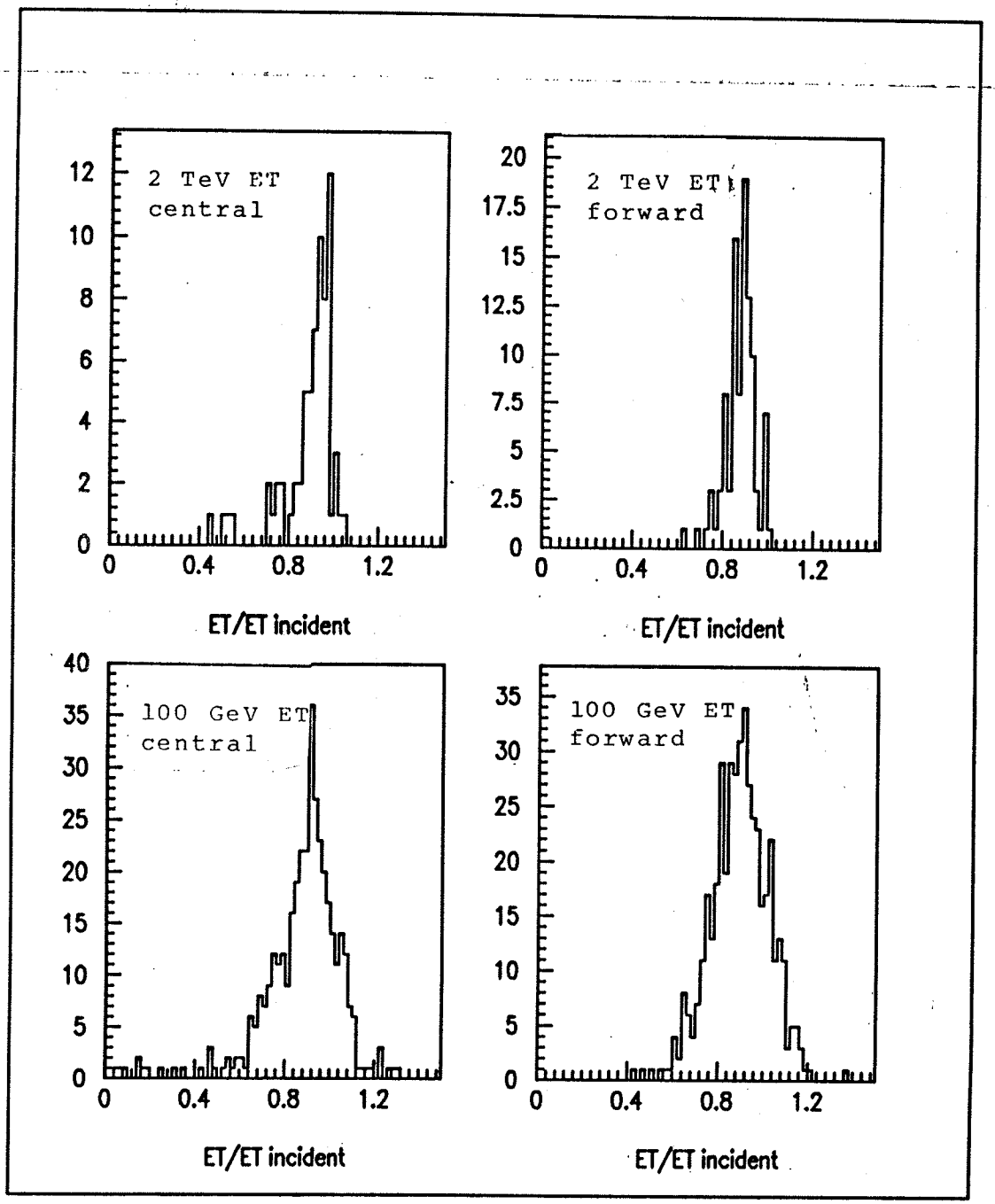

Fig. 1.6 Reconstructed E_T spectra for 100 GeV E_T and 2 TeV E_T jets in the D-Zero calorimeter.

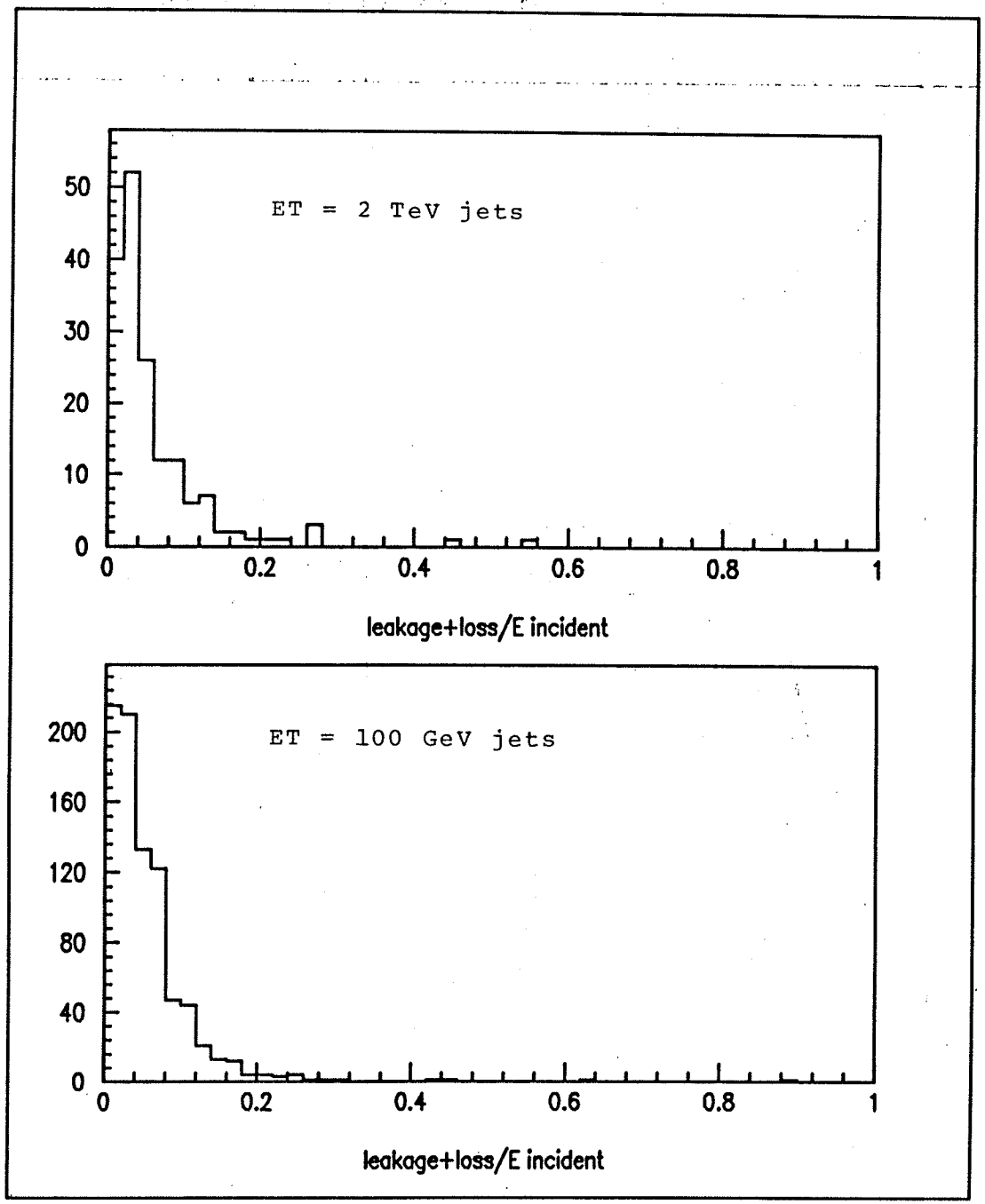

Fig. 1.7 Fraction of jet energy lost to nuclear processes and leakage from the calorimeter, for 100 GeV E_T and 2 TeV E_T jets in D-Zero.

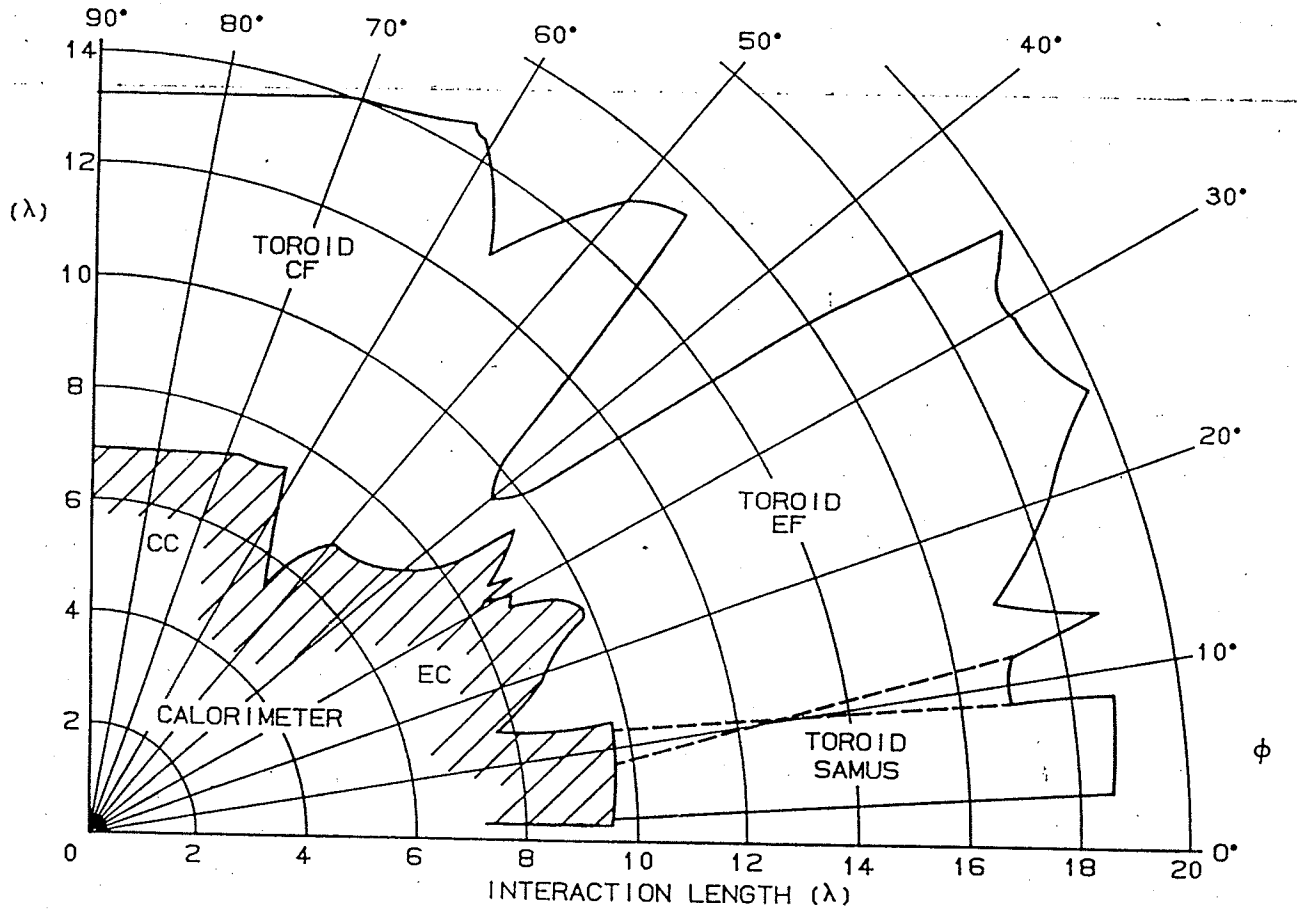

Fig. 1.8 Total interaction lengths of the calorimeter and muon system.

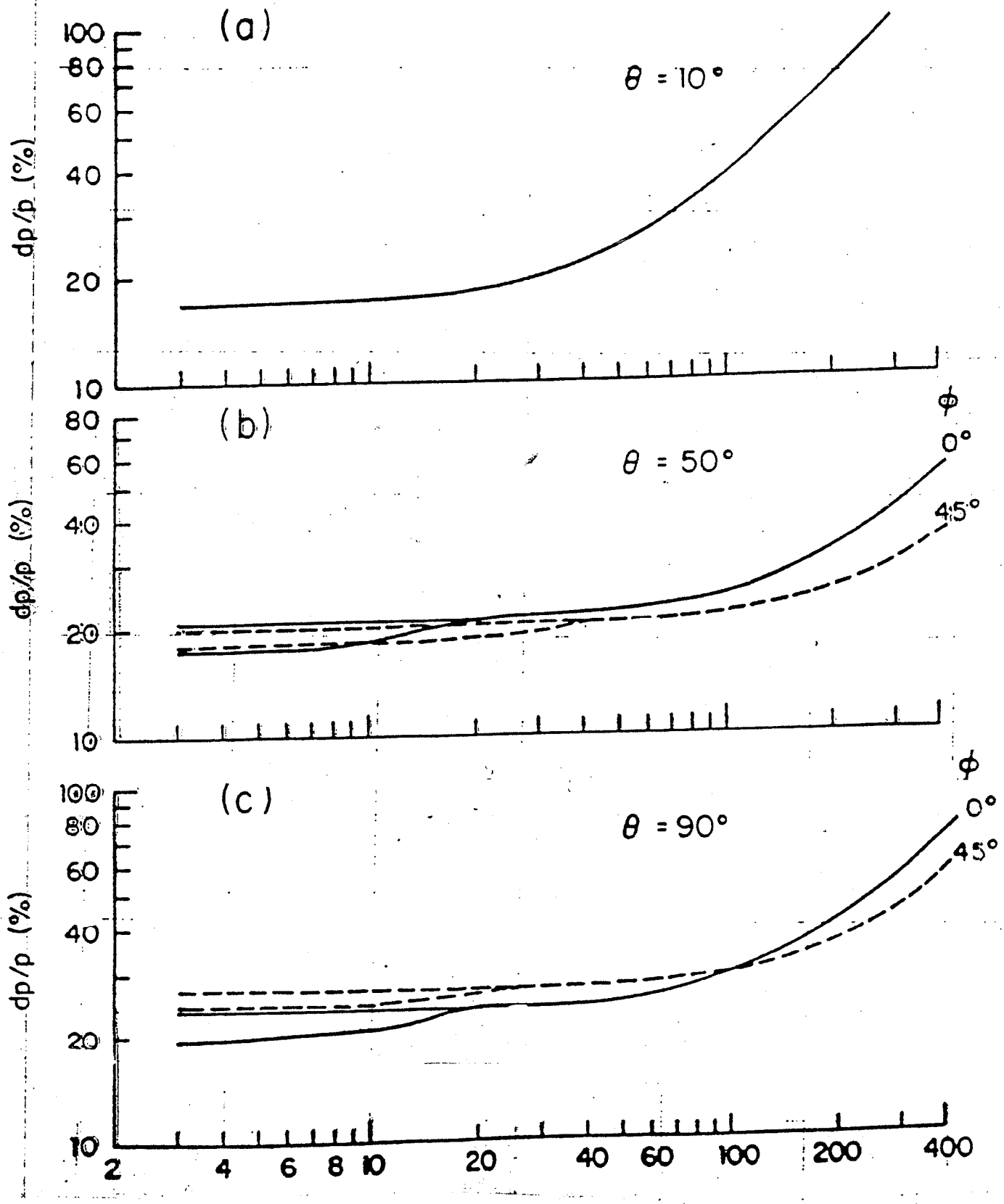

Fig. 1.9 Muon momentum resolution versus p_T for the standard D-Zero geometry. The upgraded muon detector described in the text would cause the horizontal axis to be doubled. after lepton isolations cuts.

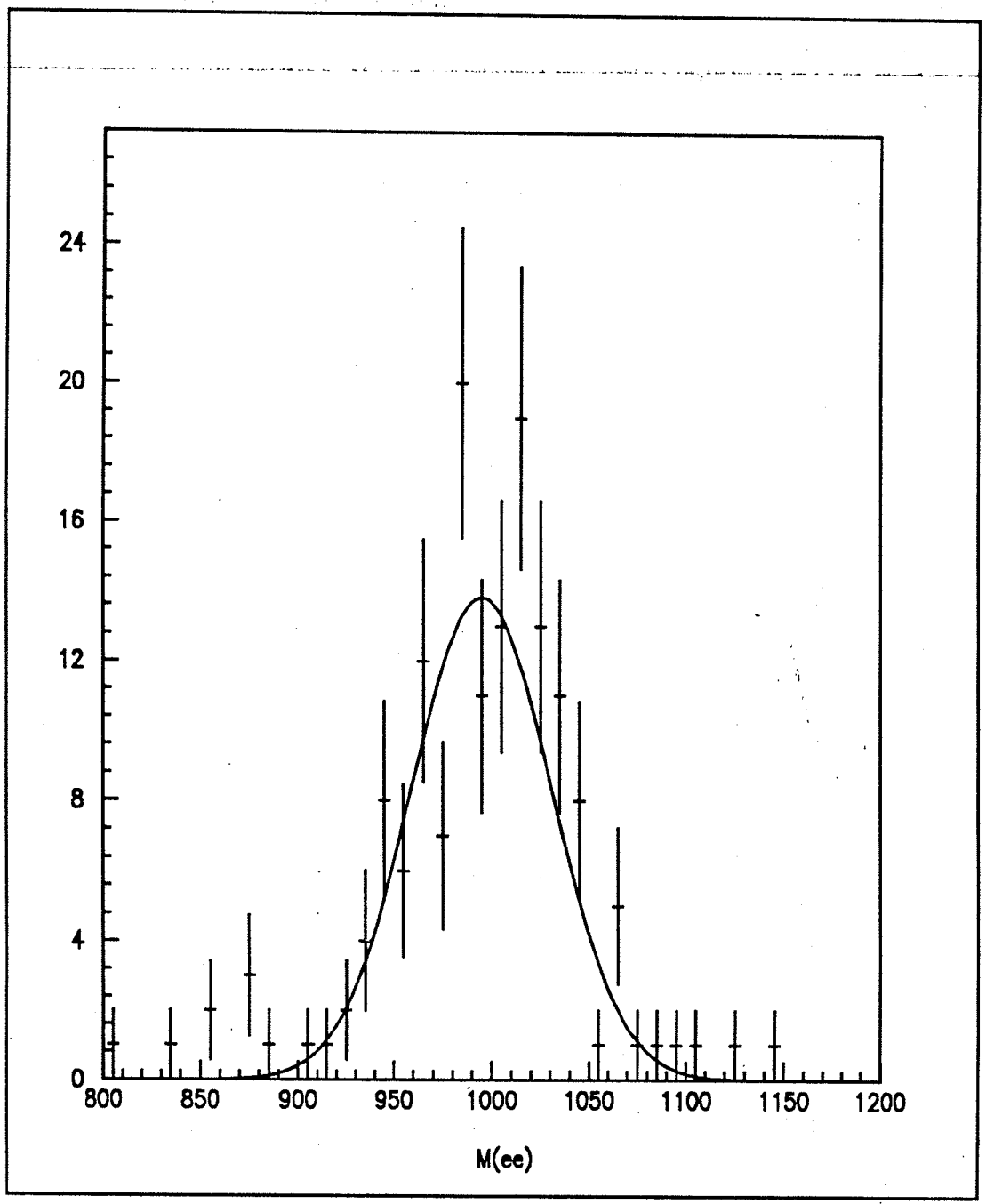

Fig. 2.1 Reconstructed ee mass spectrum for Z' decays in D-Zero, with electron $p_T >$ 20 GeV but no underlying event.

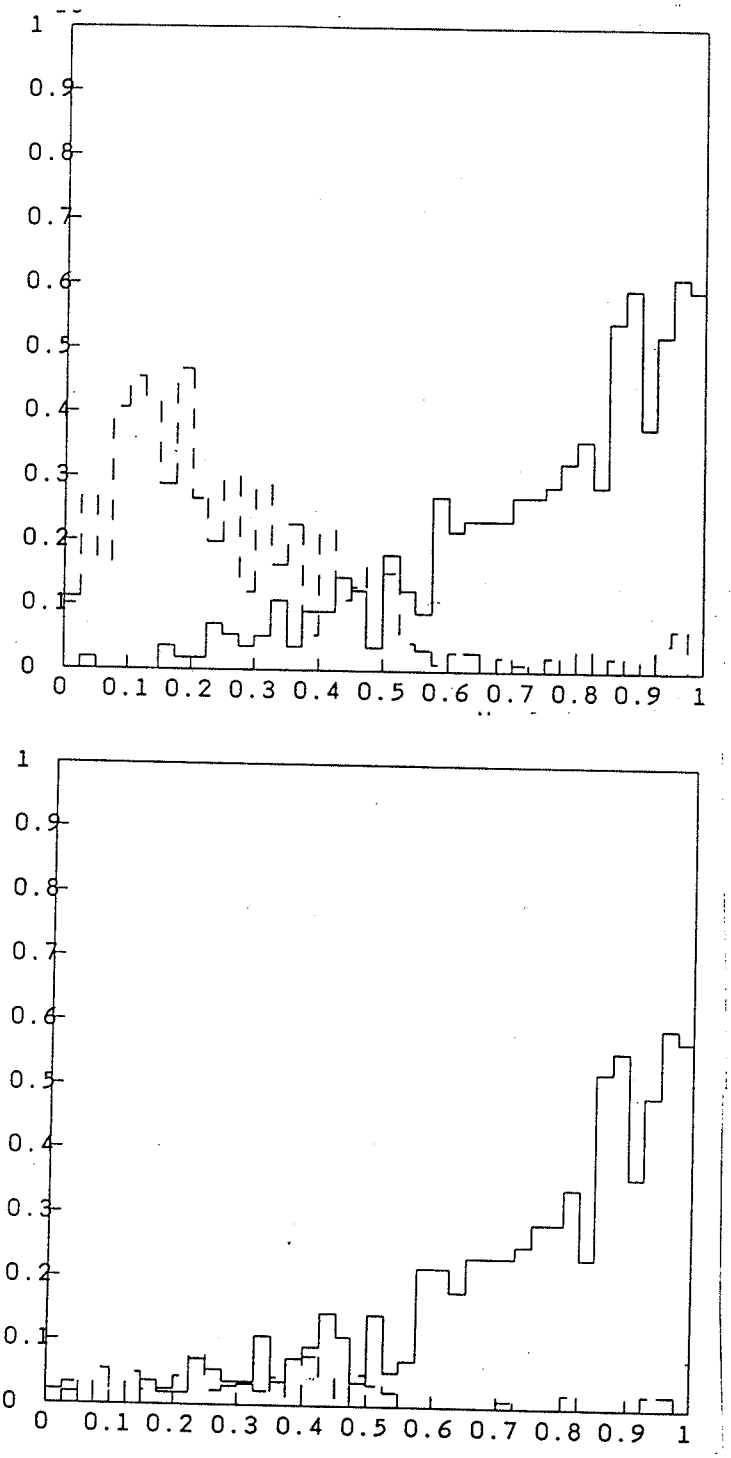

Fig. 2.2 The ratio p_{TZ1}/p_{TZ2} with $p_{TZ1} < p_{TZ2}$ for $H \rightarrow ZZ \rightarrow 4l$ events (solid) and Z + jet events (dashed) before and

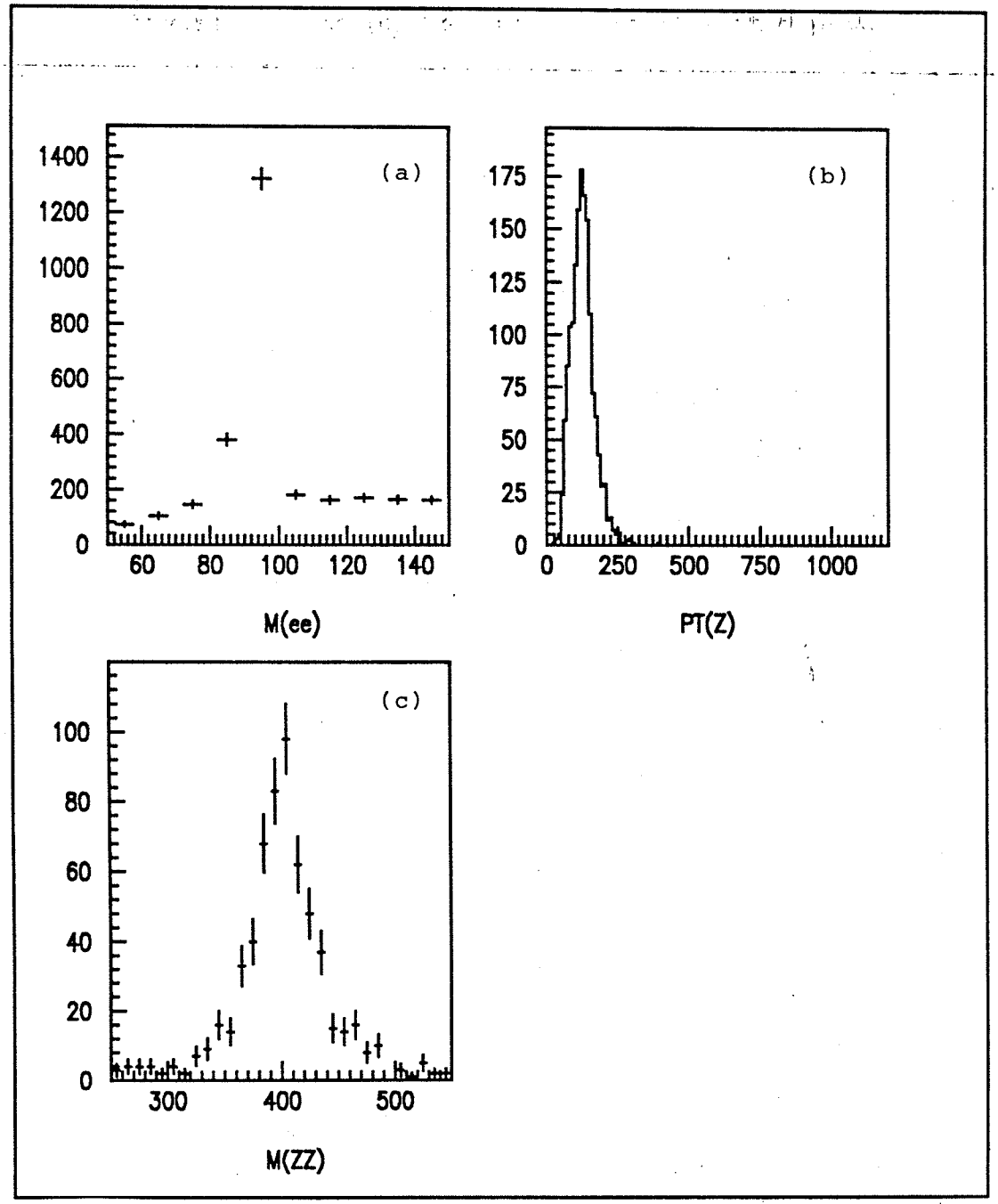

Fig. 2.3 ISAJET $H \rightarrow ZZ \rightarrow 4e$ events simulated in D-Zero with GEANT. (a) ee mass spectrum showing Z peak. Electron $p_T > 10$ GeV. (b) p_T spectrum of reconstructed Z bosons. (c) ZZ mass spectrum showing H peak.

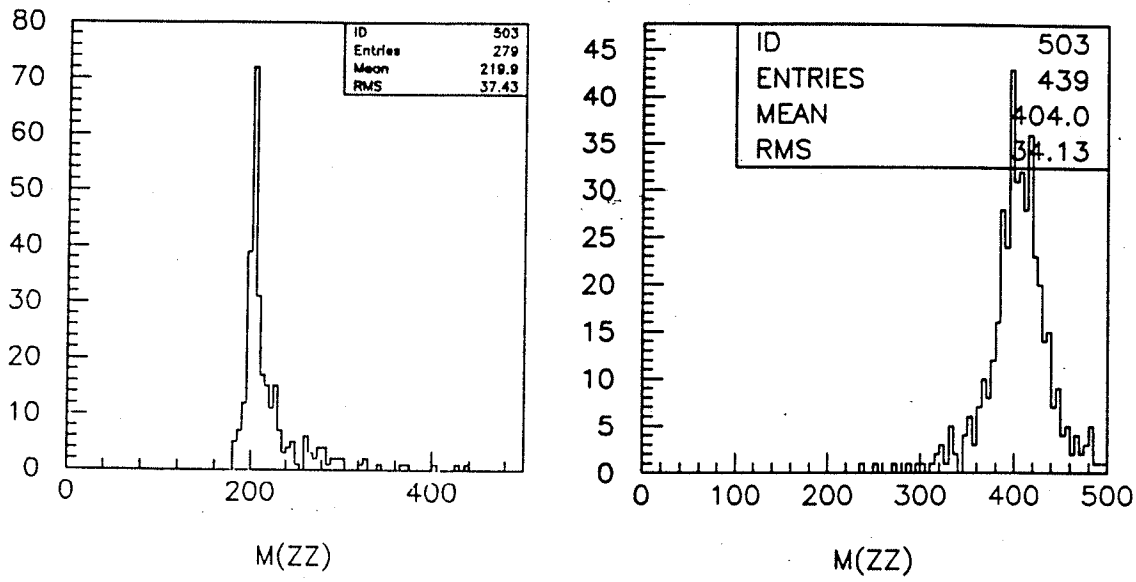

Fig. 2.4 HERWIG $H \rightarrow ZZ \rightarrow 4e$ events simulated with a "toy" calorimeter and full underlying event, for $m_H = 200$ and 400 GeV.

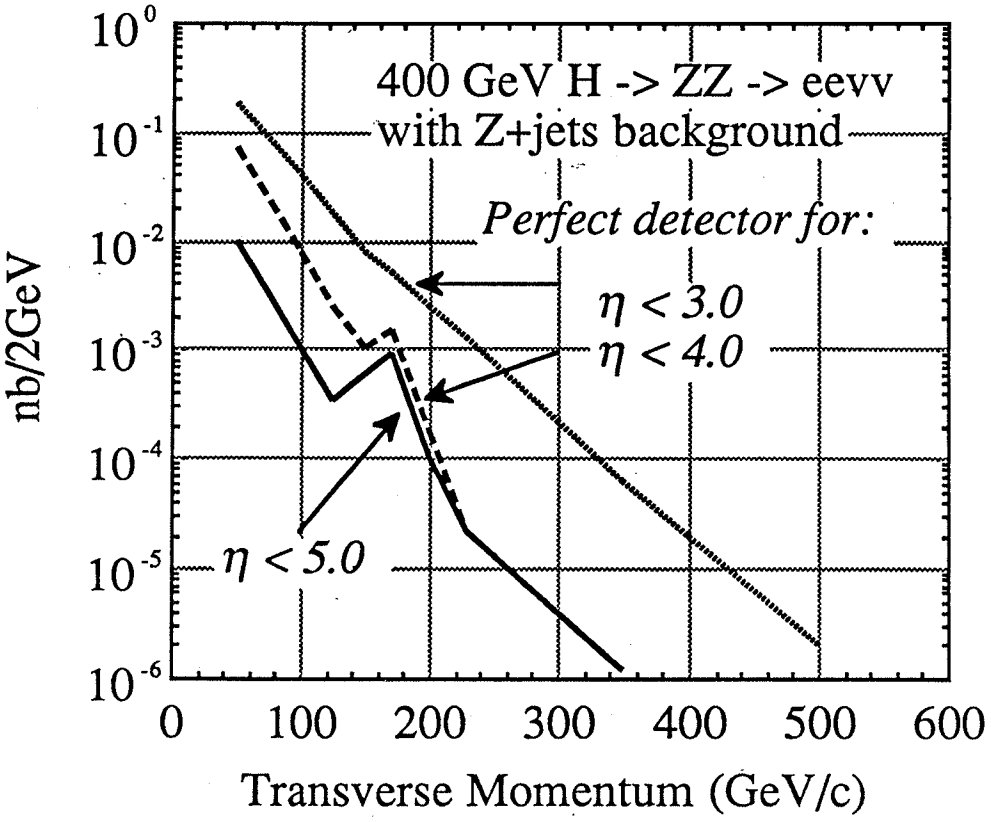

Fig. 2.6 Missing p_T spectra from reference 15 for 400 GeV $H \rightarrow ZZ \rightarrow l^+l^-\nu\nu$ and $pp \rightarrow Z$+jets, for various effective cutoffs in η coverage of the detector. D-Zero cuts off around $\eta = 4$.

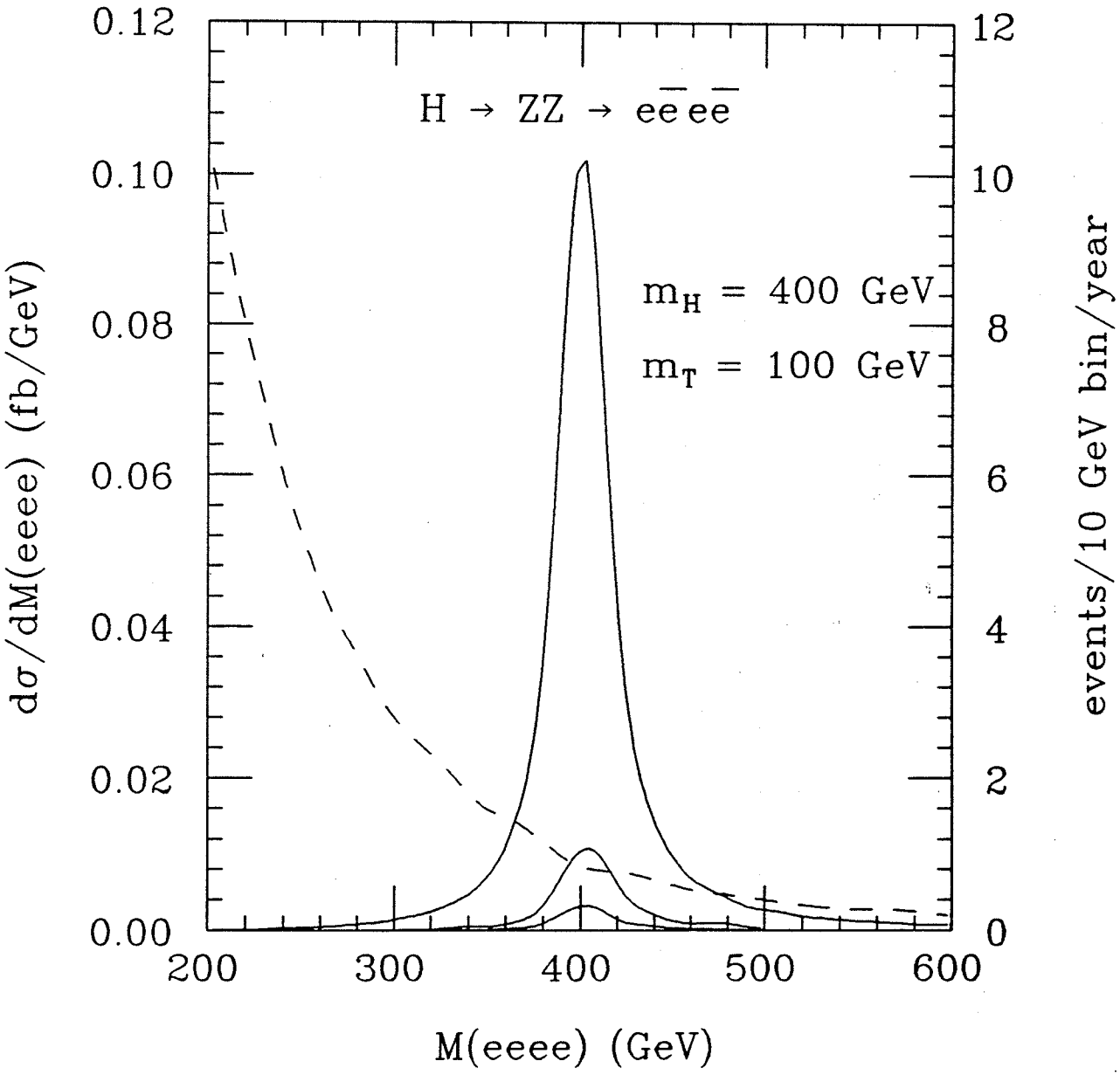

Fig. 2.5 An estimate of the ZZ continuum background to the $4e$ signal.

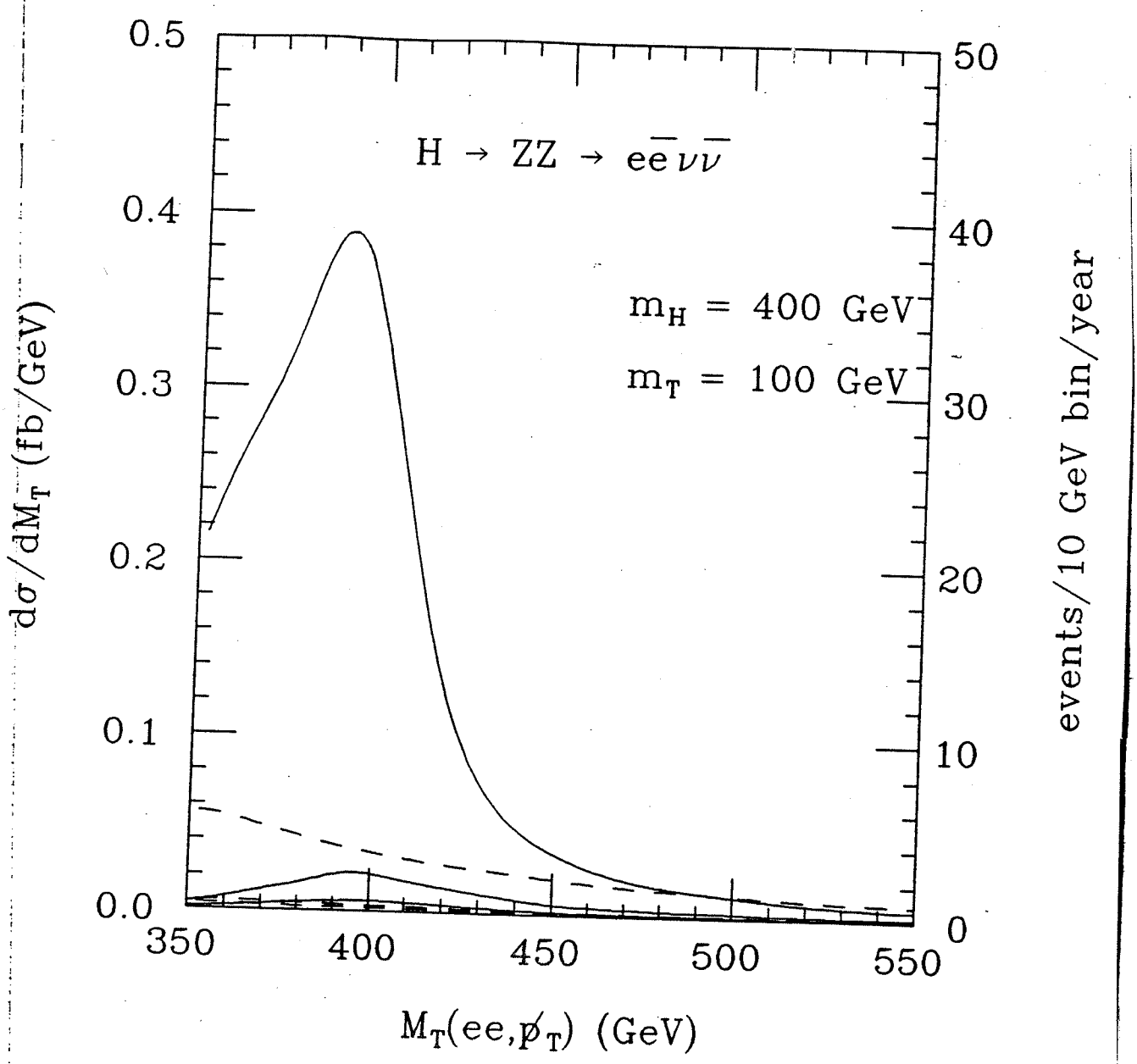

Fig. 2.7 Transverse mass spectrum for 400 GeV $H \rightarrow ZZ \rightarrow e^+e^-\nu\nu$ and $pp \rightarrow Z$+jets, for D-Zero resolutions and acceptances. Cuts used were $p_T(ee) > 150$ GeV and $p_{Tmiss} > 150$ GeV.